Ind. J. Pharm. Edu. Res., 2026; 60(1):270-282.
https://www.ijper.org

Original Article

Solid Lipid Nanoparticles of Resveratrol: Formulation, Characterization and *in vitro* Anti-Inflammatory Studies

Vedanshu Malviya[1,*], Altaf Khan[1], Sachin Padole[2], Vaibhav Thakare[1], Tushar Gajbhiye[1]

[1]Department of Pharmaceutics, School of Pharmacy, GH Raisoni University, Amravati, Maharashtra, INDIA.
[2]Department of Pharmacology, School of Pharmacy, GH Raisoni University, Amravati, Maharashtra, INDIA.

ABSTRACT

Aim: An oral administration formulation including resveratrol and solid lipid nanoparticles is the focus of this investigation. **Materials and Methods:** The resveratrol SLN was prepared utilizing oleic acid as the surfactant and hydrogenated castor oil as the lipid matrix by the high-pressure homogenization process. The FTIR and DSC techniques were used to conduct the chemical as well as physical drug interaction. Using scanning electron microscopy, the physicochemical properties of SLN were examined. Using the Assay of Cyclooxygenase and 5-lipoxygenase method, resveratrol was tested for its anti-inflammatory effects *in vitro*. Following the *in vitro* anti-inflammatory trials, a stability study was conducted. **Results:** The optimised formulation's SLN had a spherical resveratrol and a polydispersity index of 0.371±0.042, a zeta potential of -30.9±2.6 mV, a loading capacity of 1.89±0.22%, and an encapsulation efficiency of 91.80±1.7%. It exhibited good stability at 25ºC±2ºC / 60% RH±5% RH. In addition to its anti-inflammatory effects, the resveratrol exhibited a sustained release impact. **Conclusion:** Based on the results of these investigations, resveratrol in an oral formulation shows promise for less frequent dosage and improved pharmacological effects.

Keywords: Resveratrol, Solid Lipid Nanoparticles, Anti-Inflammatory Activity, Sustained Release, Stability.

Correspondence:
Prof. Vedanshu Malviya
Department of Pharmaceutics, School of Pharmacy, GH Raisoni University, Amravati-444701, Maharashtra, INDIA.
Email: vedanshumlv56@gmail.com

Received: 02-05-2025;
Revised: 19-06-2025;
Accepted: 25-08-2025.

INTRODUCTION

The essential issue with the medications is their low water solvency, which brings about unfortunate ingestion and restricted bioavailability. Strong lipid nanoparticles, a type of strong lipid-based nano-drug conveyance innovation, have thus filled in prevalence. The making of strong lipid nanoparticles was prodded by the potential for expanded drug assimilation rate.[1,2] A significant enhancement is the use of solid lipid nanoparticles, which shield the encapsulated pharmaceuticals from stomach degradation and offer tremendous flexibility in managing drug release due to the solid lipid matrix. According to previous study solid lipid nanoparticles typically have a biodegradable and bio compatible solid lipid core and an exterior shell covered with a nonhazardous surfactant or co-surfactant.[3,4] Solid lipids boost medication solubilization and dissolution in the intestinal lumen, lymphatic transport, gastrointestinal permeability, and stomach emptying rate, which in turn enhances drug absorption.[5,6] When it comes to the stability and production of solid lipid nanoparticles, two crucial criteria are particle size and PDI.[7] The manufacturing process and the composition of the particles are the primary determinants of these properties.

The polyphenolic phytoalexin resveratrol, ($C_{14}H_{12}O_3$), is abundant in red grapes and has various potential medical advantages, including reduced risk of hyperlipidemia, diabetes, atherosclerosis, fatty liver, premature ageing, and cancer.[8] Additionally, it blocks the action of certain DNA helicases and prevents platelet aggregation. It is synthesised in plants by the stilbene synthase enzyme and is also known as a stilbenoid, a derivative of stilbene. With a 95% success rate in avoiding lipid peroxidation, resveratrol shows promise as a potent antioxidant. It contains epicatechins, gallic and ellagic acids, and a significant capacity to scavenge peroxyl radicals. Protecting cells from oxidative damage is one of resveratrol's antioxidant functions.[9]

MATERIALS AND METHODS

Yarrowchem Pvt. Ltd., of Mumbai supplied the resveratrol, Corel Pharma Chem of Gujarat provided us with the hydrogenated castor oil, Varun Biochemicals of Mumbai provided with the soy lecithin and S.D. Fine Chem of Mumbai helped us out for procuring oleic acid and Span 80. Everything else that was employed was of an analytical grade chemical or reagent.

DOI: 10.5530/ijper.20261895

Methods

Drug- Excipients Compatibility Study

We used FT-IR and DSC to investigate the drug-excipient interaction.

Fourier-Transform Infrared Spectroscopy

The traditional KBr plate method, a widely used technique in FTIR research, was carefully employed to analyze both the compound and excipient. This method was chosen to delve into the intricate drug-polymer interaction and unveil any potential physical or chemical modifications that could arise during the formulation process. To achieve this, the excipient and pure powders were meticulously combined in a precise 1:1 ratio with potassium bromide, leading to the creation of a minute pellet by subjecting the mixture to intense pressure using a hydraulic press. Subsequently, the FT-IR analysis was expertly conducted across the expansive 400-4000 cm^{-1} frequency range. By scrutinizing and comparing the most notable peaks identified in the spectra with the standard FTIR, a comprehensive understanding of the molecular interactions and compositional changes was gained.[10]

DSC Study

To conduct the Differential Scanning Calorimetry (DSC) investigation thoroughly, we meticulously analyzed thermograms obtained from the pure drug and a physical blend comprising the drug and different polymers. This meticulous examination was crucial as it provided insights into potential interactions between the drug and the polymers. Furthermore, in their methodology, they meticulously selected a specific heating rate of 20°C/min to steadily heat the samples from 50°C to 400°C using the Differential Scanning Calorimeter apparatus, a critical step to ensure accurate and reliable results for the study.[11]

Standard Calibration Curve

A UV spectrophotometer was meticulously utilized to meticulously conduct the standard calibration curve of resveratrol, which involved using a precise phosphate buffer solution with a pH level carefully maintained at 7.4. With exacting precision, varying volumes of 0.5, 1, 1.5, 2, 2.5, 3, 3.5, 4, 4.5, and 5 mL were meticulously transferred using a pipette from the existing 100 µg/mL concentration solution into separate 10 mL volumetric flasks. These volumes were then meticulously complemented to the 10 mL mark with the addition of phosphate buffer 7.4, effectively creating a series of final concentrations ranging from 5 µg/mL to 50 µg/mL. For the pharmacological assessment, the concentration's absorbance at a precise frequency of 304 nm was meticulously determined to ensure accurate and reliable results.[12]

Preparation of Nanoparticles

In Table 1, we can see the complete process of making solid lipid nanoparticles, where A represents the overall lipid concentration, B the liquid lipid concentration, and C the surfactant concentration. The hydrogenated castor oil was melted in a china dish at 80°C with the addition of soya lecithin and 2% oleic acid. Distilled water was used to make the aqueous phase. After the two components were combined at the same temperature, they were stirred for 1 min at 15,000 rpm to create a homogeneous emulsion. This mixture was then passed through a High-Pressure Homogenizer (HPH) while maintaining a pressure of 500 bars. The different parameters of the resulting SLN were assessed. The nanosuspensions that were made were combined with mannitol, a cryoprotective agent, at a ratio of 50% by weight to the medication, and then frozen at a temperature close to -20°C for 24 hr.[13-15]

Evaluation Parameters

Physiological Evaluations

Utilizing Dynamic light dispersing, a Zetasizer Nano ZS 90 from Malvern Ltd. UK was utilized to quantify the molecule size and PDI of the NLC scattering. A 1:10 proportion of deionized water to all examples was utilized to accomplish the ideal 100-200 Kilo Counts each Second (KCPS) for estimations. For each cluster of nanoparticles, we decided their normal size and standard deviation (3 total). Electrophoretic portability (Zetasizer Nano ZS 90, Malvern Ltd., UK) was utilized to assess the zeta capability of the NLC scattering. Deionized water was utilized to weaken all examples at a 1:10 proportion. We figured the normal zeta potential and standard deviation σ for each bunch of nanoparticles (n=3).[16]

Entrapment Efficiency (%) and Drug Loading

Using centrifugation to separate the resveratrol-loaded nanoparticles from the liquid containing free resveratrol allowed us to determine the quantity of resveratrol entrapped in the particles. Subsequently, after evaporating the solvent, the resulting suspension was subjected to centrifugation. The concentration of free resveratrol in the resultant supernatant was analyzed utilizing a UV spectrophotometer set at 304 nm. This process of determining the quantity of drug trapped within nanoparticles involved subtracting the amount of drug present in the supernatant from the total amount of drug utilized during the formulation, thus enabling accurate calculation and evaluation of drug encapsulation efficiency.[16] This formula was used to determine the percentage of entrapment efficiency.

$$EE\ \% = \frac{\text{Quantity of medication added} - \text{Amount of medicament in supernatant}}{\text{Quantity of medication added}} \times 100$$

$$\%\ \text{Drug Loading} = \frac{\text{Total amount of medicament entrapped in SLN}}{\text{Total SLN weight}} \times 100$$

Surface Morphology

While conducting a thorough examination of the advanced Solid Lipid Nanoparticle (SLN), we utilized scanning electron microscopy to assess its surface morphology. To enhance the

visualization, a platinum particle falter was employed for 300 sec to even disperse the SLNs. Images of the SLN cluster were then captured using a back-scattered electron detector on a Joel JSM 6360 scanning electron microscope located in the USA, operating at a speed acceleration voltage of 15 kV. This detailed imaging technique provided valuable insights into the structural characteristics of the SLN cluster at a microscopic level.

In vitro Drug Release Study

In our experimental procedure, we employed the dissolution apparatus known as the USP (2nd Type), operating it under specific conditions of temperature (37±2°C) and rotation speed (50 rpm) for a duration of 12 hr. This process was conducted using two distinct solvents for testing purposes: firstly, 0.1 N HCl, and secondly, a phosphate buffer solution with a pH of 6.8. This permitted us to evaluate what pH meant for the medication discharge exhibit from SLN. A capsule containing the SLN was placed in the dissolving vessel. The drug concentration was determined by spectrophotometry at 304 nm after 5 mL aliquots were taken from the dissolving media at different times for up to 24 hr, filtered using Whatman filter paper, and then analysed. It was necessary to replenish the dissolving medium in the dissolution vessel after removing the aliquots so that the sink condition could be maintained.[17]

Ex vivo permeability study

The local abattoir supplied freshly chopped goat intestine. The everted goat intestine model was used to assess the permeability research of the produced SLN via the goat gut. Using a syringe, 1 cc of phosphate buffer, pH 6.8, was added to the isolated intestine after clamping and suturing one end of the glass rod that had been everted. Then, the end that was closest to the needle was snugly fastened with silk suture. The resulting sac was then placed in an incubator at 37°C with a solution of bulk resveratrol (effective concentration 5 µg/mL) and at 37±4°C with a solution of resveratrol SLN (effective concentration 5 µg/mL). After half an hour, the fluid within the lumen was analyzed using spectrophotometry at 304 nm to determine the medicine content.[18]

Histological Examination

For the histological evaluation, we used all of the skin tissues that were utilised in the *ex vivo* study. We took specimens from both the treated and non-treated tissues in each group and preserved them in a 10% (v/v) formalin solution.[18]

Kinetics Study

In order to determine the optimal medication discharge energy and plan the delivery process using pre-arranged strong lipid nanoparticles, various models were employed to analyze drug discharge information. These models included zero-order, first-order, Higuchi, and the Korsemeyer-Peppas models, with the relationship between the log of the percentage cumulative drug release and the log of time being carefully assessed. By fitting the drug discharge data to these models, a comprehensive understanding of the drug release kinetics was obtained to guide the implementation of the delivery system effectively.[19]

X-ray Diffraction Study (XRD)

The X-ray diffraction frequencies of resveratrol and the synthesized nanoparticles were meticulously determined by employing a sophisticated X-ray diffractometer operating at specific parameters-45 kV and 40 mA-to ensure accurate readings. This device was set to continuous scan mode across a precise 2θ range spanning from 20° to 80°. The analysis further delved into the examination of relative intensity (I/I0) and interplanar distance (d), aligning these aspects with the corresponding 2θ values for a comprehensive and detailed investigation.[20,21]

Anti-Inflammatory Activity

Lymphocyte Culture Preparation

In our process of cultivating human peripheral lymphocytes, the growth medium played a crucial role. For this purpose, we employed RPMI 1640 (HIMEDIA) material supplemented with essential nutrients like streptomycin and penicillin, along with fetal calf serum to create a conducive environment for cell proliferation. Phytohemagglutinin (HIMEDIA) was used to mediate cell growth. Following the addition of 1×10^{1} cells/mL of plasma, the culture was cleaned using Sartorios cellulose acetate with 0.2 µm pores and then allowed to grow for 72 hr. After activating the culture with 1µl of lipopolysaccharide, it was incubated for 24 hr. Diclofenac, the pure medication, and the optimized formulation were incubated for 24 hr after activation. To separate the sediment, they must next be spun in a centrifuge for 10 min at 6,000 rpm. After the supernatant was discarded, 50 µl of cell lysis buffer was incorporated, and the mixture was centrifuged once more for 10 min at 6000 rpm.[22]

Assay (Investigation) of Cyclooxygenase

A cyclooxygenase examination was done utilizing the catalyst, hemoglobin, glutathione, and Tris-HCl cradle. The blend was then brooded for 20 min at 37°C with 0.2 mL of 10% arachidonic corrosive and TCA in 1N HCl added. The fluid was then brought to a stew for 20 min with 0.2 mL of TBA added. When the combination has cooled, axis it for 3 min at 1000 rpm. The supernatant was utilized to test the COX movement at 632 nm.[22]

Assay (Investigation) of 5-lipoxygenase

The investigation on lipoxygenase was meticulously conducted by combining 70 mg of linoleic acid with 4 mL of non-oxygenated water, proportionally between 20. Additional sodium hydroxide (0.5 N) and more non-oxygenated water were essential to reach

a final volume of 25 mL. Once prepared, the mixture underwent division into half-milliliter aliquots, followed by a thorough nitrogen wash and subsequent freezing. The ensuing reaction was performed within a quartz cuvette with a 1 cm optical path length at a constant temperature of 25°C. The necessary components for the mix included sodium linoleate (0.2 mL), Tris buffer medium (2.75 mL at pH 7.4), and the crucial testing enzyme (50 mL). All these elements were integral for determining the Optical Density (OD) at 234nm, a pivotal step in the experimental process.[22] We used the following equation to get the inhibition percentage:

$$\% \text{ Inhibition } = \frac{\text{Optical thickness (control)} - \text{Optical thickness (absorbance)}}{\text{Optical thickness (control)}} \times 100$$

Inhibition of Protein Denaturation

After being incubated for 15 to 20 min at 37°C±2°C in a water bath, the reaction combinations were then heated to 70°C and maintained for 5 min. The reaction mixture was then allowed to cool at room temperature for 15 min. A colorimeter was used for gauging the reaction mixture's absorbance at 680 nm before and after denaturation for each concentration. Each test was run three times, and the overall absorbance was calculated. We applied the following formula to determine the protein inhibition percentage in relation to the control.[23]

$$\frac{\text{Absorbance of Control} - \text{Absorbance of Test}}{\text{Absorbance of Control}} \times 100$$

Statistical Analysis

All collected data underwent rigorous statistical analysis utilizing SPSS version 20 (IBM, Somers, NY, USA). Descriptive data, comprising mean values accompanied by the standard error of the mean, were meticulously documented. In order to assess the discrepancy in inhibition percentages across the diverse groups, an independent sample t-test was implemented. Subsequently, a significance level of 0.05 was chosen, and any observed differences exceeding this threshold were deemed statistically meaningful, signifying a crucial finding in the context of the study's investigative goals and objectives.[24]

Stability Study

Stability testing is an essential process that must be conducted to determine the most suitable storage conditions, recommended retest intervals, and optimal shelf lives for a medicinal ingredient or medication product. This testing is imperative not only for assessing the product itself but also for monitoring how its quality evolves over time due to a variety of environmental factors such as light exposure, temperature fluctuations, and humidity levels. By analyzing the impact of these conditions, stability testing provides valuable insights into the long-term stability, efficacy, and safety of the pharmaceutical product, ensuring its quality and effectiveness throughout its shelf life.[24] The formulation's stability was tested for three months at room temperature (25°C±2°C/60% RH±5% RH) and accelerated conditions (40°C±2°C/75% RH±5% RH). We examined the optimized formulation's entrapment efficiency, zeta potential, particle size, and appearance.[25-27]

RESULTS

Drug- Excipient Compatibility Study

FTIR

Both the pure drug and the combination comprising the drug and the largest number of excipients revealed comparable patterns and fundamental peaks in the FTIR spectra. The FTIR data, as seen in Figure 1, showed the peaks that stand for the functional groups. Both stretching and bending peaks were

Table 1: Formulation Chart of Solid Lipid Nanoparticles of Resveratrol.

Sl. No.	Batch	Drug	A (mg)	B (%)	C (%)
1	F1	500	1.5	30	1
2	F2	500	1.5	40	1
3	F3	500	2	40	1.5
4	F4	500	1	20	0.5
5	F5	500	2	20	0.5
6	F6	500	2	20	1.5
7	F7	500	1	40	1.5
8	F8	500	1.5	30	1.5
9	F9	500	1	30	1
10	F10	500	1.5	30	0.5
11	F11	500	1	40	0.5
12	F12	500	1.5	20	1
13	F13	500	1	20	1.5
14	F14	500	2	40	0.5
15	F15	500	2	30	1

seen in the pure resveratrol medication. The C-Br stretching is represented by 524.66-624.96 cm^{-1}, the C-Cl stretching by 67026-833.28 cm^{-1}, the =C-H bending by 995.31 cm^{-1}, the -C-H bending by 1388.81-1458.25 cm^{-1}, the -C=C stretching by 1458.25-1597.13 cm^{-1}, the -C≡C stretching by 2152.65-2199.85 cm^{-1}, the -C-H stretching by 2893.35-3032.23 cm^{-1}, the -N-H stretching by 3309.94 cm^{-1}, and the O-H stretching by 3742.06 cm^{-1}, respectively. The FTIR data from the optimised formulation also showed peaks that did not alter, vanish, or mismatch from the pure drug FTIR values. These findings suggest that there was no physical or chemical incompatibility between the pure medicine resveratrol and the excipients utilised.

DSC

When testing formulations for drug-excipient interactions, DSC is an invaluable tool. The melting process peaked at 267.24°C for the bulk mass of pure resveratrol. DSC analysis of freeze-dried SLN revealed an endotherm at 265.59°C, which is likely due to the resveratrol melting point. As amorphous an area containing molecularly dispersed resveratrol forms, the sharp to wide DSC peak changes. These results can be seen in Figure 1.

Standard Calibration Curve

The UV absorbance experiment involved analyzing a resveratrol standard solution within a buffer solution with a specific pH level of 7.4. The results highlighted a clear trend of linearity at a specific wavelength (λ_{max} 304nm) across various drug concentrations, spanning from 10 to 50 µg/mL. By utilizing a carefully calculated slope equation (y=0.0179x-0.003) and achieving a high R2 value of 0.9995, the relationship between concentration and absorbance was clearly established. Further insights can be gleaned from Figure 2a, where the absorbance values and the resultant standard curve are impeccably presented for visual interpretation.

Evaluation Parameters

Physiological Parameters

Table 2 displays the results for the synthesised SLNs, which vary from 81.14±3.9 to 146.0±7.2 nm in particle size, 0.34±0.029 to 0.471±0.042 in Polydispersity Index (PDI) and -20.7±2.1 to -32.1±2.5 mV in Zeta Potential (ZP).

Entrapment Efficiency (%) and Drug Loading

How much of the active ingredient gets absorbed in the formulation as a proportion of the total amount of resveratrol added is called entrapment efficiency. Absorbance measurements

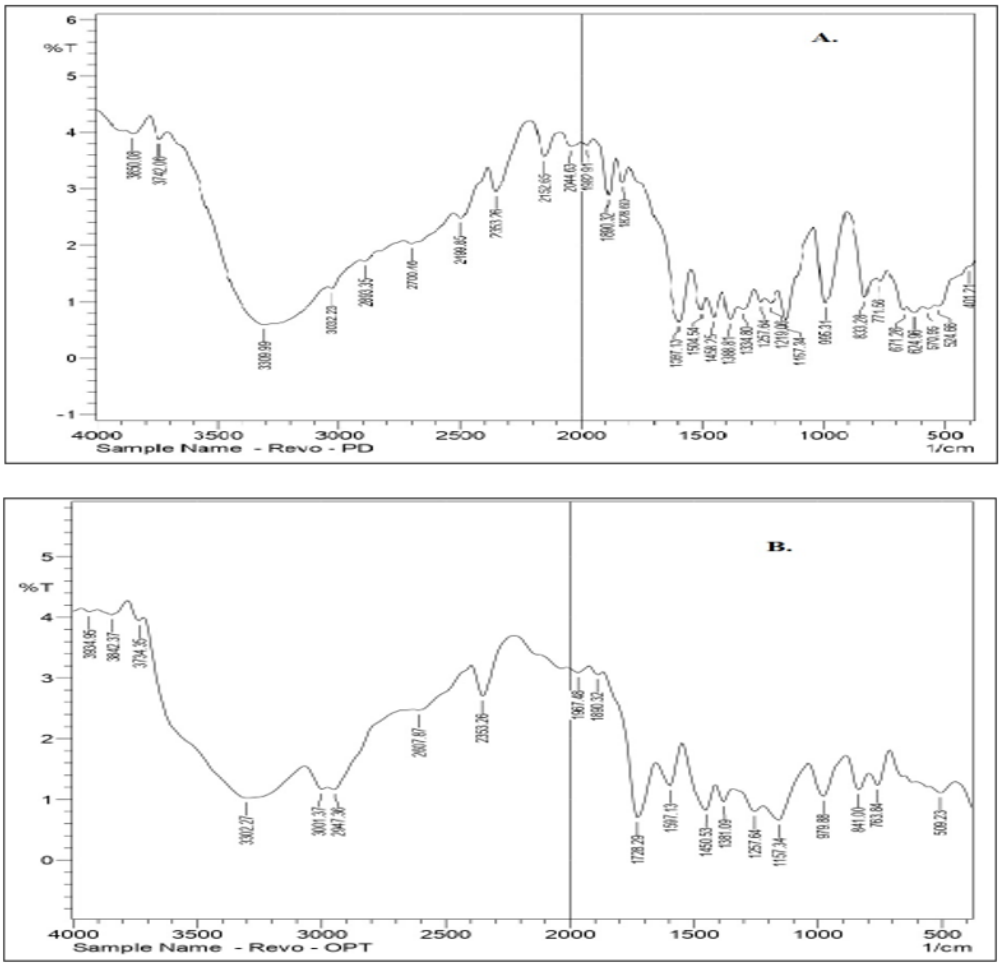

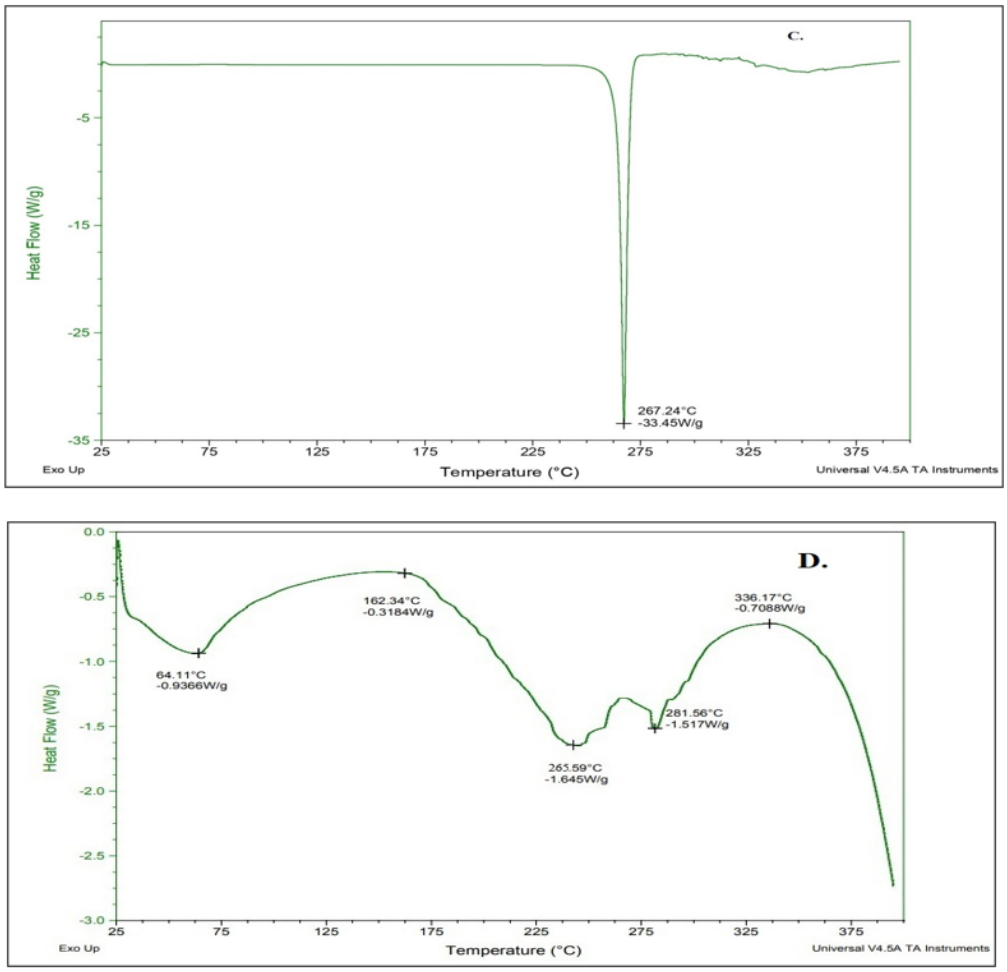

Figure 1: A) Results for FTIR of pure resveratrol, B) Results for FTIR of optimized formulation, C) Results for DSC of pure resveratrol, D) Results for DSC of optimized formulation.

Table 2: Particle size, Polydispersity Index and Zeta Potential of the prepared Batches.

Formulation Code	Particle Size (nm)	Polydispersity Index (PDI)	Zeta Potential (mV)
F1	81.14±3.9	0.311±0.039	-28.1±2.6
F2	84.24±5.3	0.460±0.038	-28.4±2.2
F3	149.9±5.9	0.371±0.042	-30.9±2.6
F4	139.5±6.01	0.392±0.06	-31.6±2.7
F5	141.5±7.5	0.342±0.029	-32.1±2.5
F6	142.9±5.8	0.42±0.041	-24.2±3.0
F7	146.0±7.2	0.410±0.040	-27.4±3.1
F8	121.6±6.4	0.471±0.042	-31.3±2.6
F9	110.1±4.3	0.352±0.035	-30.9±2.0
F10	119.8±6.8	0.341±0.032	-21.7±2.4
F11	108.1±8.02	0.436±0.041	-26.4±2.8
F12	120.4±7.4	0.34±0.029	-28.2±3.1
F13	139.5±7.04	0.394±0.037	-29.4±2.3
F14	137.2±7.9	0.381±0.036	-24.9±1.5
F15	103.9±6.4	0.34±0.031	-20.7±2.1

demonstrated resveratrol concentration absorption, and a linear equation using the standard calibration curve determined the resveratrol-loaded SLN's absorption efficiency. According to Table 3, the efficiency of drug entrapment reached its peak within the absorption efficiency range of 81.2±1.4 to 91.8±1.7%. The drug's release rate is expected to be enhanced due to its high absorption efficiency. To determine the drug loading, we divided the entire solution volume by the quantity of resveratrol absorbed by the nanoparticle system. A medication loading ranging from 1.34±0.44% to 1.89±0.22% was produced by this computation. The results show that F3 had the highest drug entrapment (91.8±1.7%), followed by drug loading (1.89±0.22%). In an ideal world, a nanoparticulate system would have a large loading capacity, allowing for the reduction of drug delivery material.

Surface Morphology

A transmission electron microscope and an optical microscope were used to study the SLN particle's morphology. Figure 3 shows that the resveratrol-loaded SLN particles did not aggregate and had a smooth, spherical surface. This discovery implies that, irrespective of the lipid type, nanoparticles carried by lipids have a spherical shape and a flat surface. F3 optimised resveratrol nanoparticles have a size of 149.9±5.9 nanometers. According to these findings, nano lipids with lower particle sizes are formed by the oleic acid concentration of NLC.

In vitro Study

Figure 2b displays the *in vitro* release curves of drug-loaded nanoparticles of the SLN type. An initial stage of drug burst release and subsequent sustained release at a steady pace characterised the biphasic drug release pattern for SLN drug release. The release rate accelerated as the particle size dropped because nanoparticles' specific surface areas increased. Consequently, the nanoparticles of optimised batch F3 exhibited the quickest initial release rate, which was due to their smaller size and increased oleic acid content. The range in which the drug release was found to be 81.563±1.58 to 98.473±0.842

Ex vivo Permeability Study

The findings of the *ex vivo* permeation investigations are shown in Figure 2c. While the pure drug solution demonstrated a release rate of 88.96±1.79%, the SLN F3 formulation outperformed pure resveratrol with a release rate of 76.65±1.58% after 24 hr. The effectiveness of the SLN formulation in enhancing drug delivery

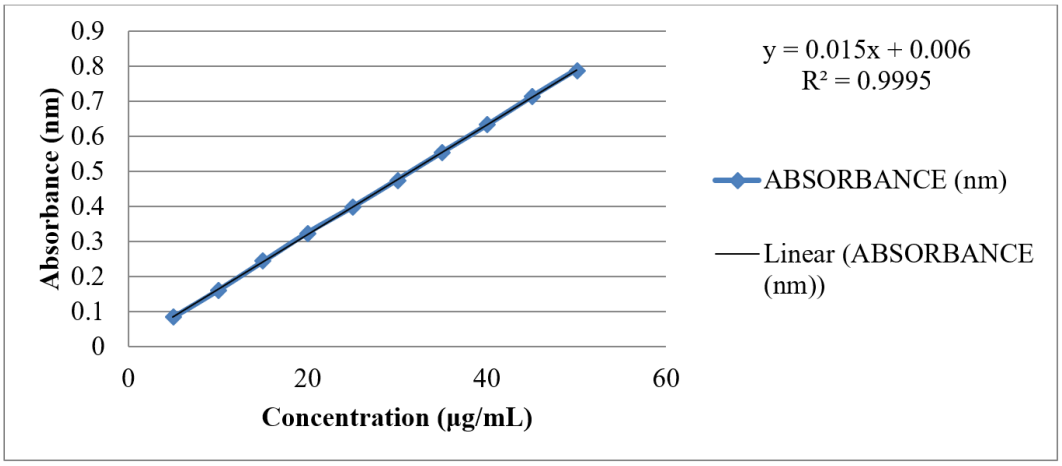

Figure 2a: Standard calibration curve of resveratrol.

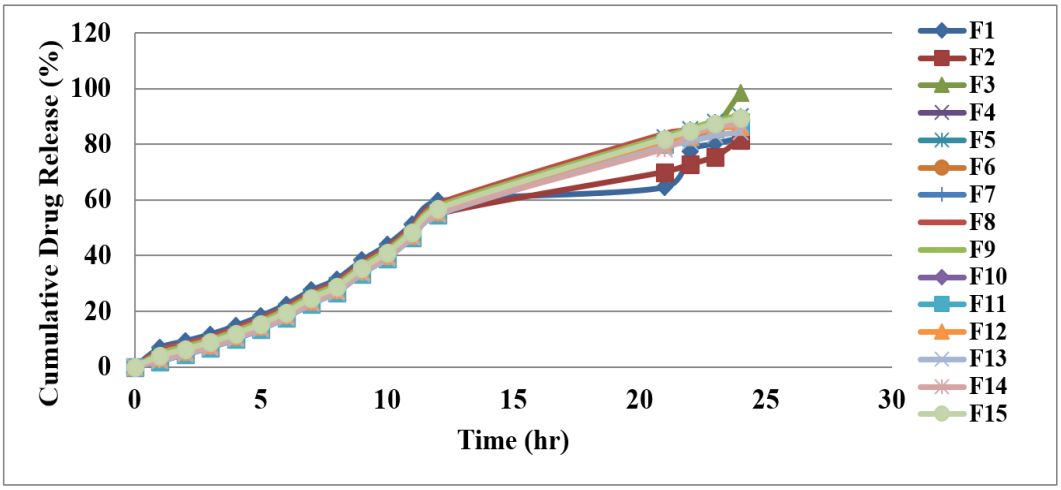

Figure 2b: *In vitro* drug release of SLN of resveratrol.

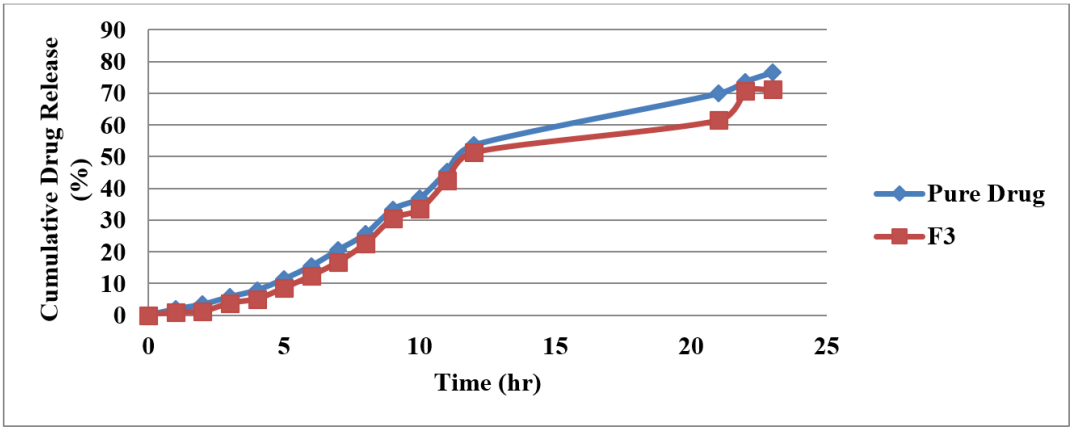

Figure 2c: *Ex vivo* study of drug release pattern from the intestine of Goat.

may be assessed by comparing the pure medication with the SLN-loaded version in *ex vivo* permeability experiments.

Histopathological Study

If the developed product caused any pathological alterations in the gut tissues, a histopathology examination would be necessary to identify them. There were no visible symptoms of irritation (reddening and swelling) on intestinal tissue while administering either the standard or resveratrol-loaded SLN formulations. Figure 4 displays histological sections stained with hematoxylin and eosin from the untreated, placebo-SLN-treated, and resveratrol-loaded intestinal tissues, respectively. Skin tolerability of SLN was confirmed by the fact that SLN-treated samples of intestinal tissues showed no abnormalities in normal histology or inflammation.

Kinetics Study

The manner of diffusion through the formulation to the receiving medium plays a major role in the *in vitro* release of the active ingredient. The kind of pharmaceutical formulation has a significant impact on the rate of release of the active ingredient, as demonstrated by the data obtained from UV-vis spectrometry. The lipid nanoparticles added to the SLN type formulation made the substrate more lipophilic, indicating a marginally greater affinity for the included nanoparticles. To determine the drug release mechanism, the profiles were also matched to several mathematical models. The release profile from SLN, which followed a non-fickian diffusion of drug release, best matched the first-order kinetics.

X-ray Diffraction Study (XRD)

Research using XRD showed that the amorphous resveratrol in SLNs is reduced because these nanoparticles are prepared using high-energy processing techniques that can produce heat and shear forces, such as high-pressure homogenization. There is less crystallinity in XRD patterns when the material is in an amorphous condition because there is no longer any long-range order and

Table 3: Entrapment Efficiency (%) and Drug Loading Capacity.

Formulation Code	Entrapment Efficiency (%)	Loading Capacity (%)
F1	84.23±1.21	1.48±0.15
F2	90.6±1.6	1.34±0.52
F3	91.8±1.7	1.89±0.22
F4	81.2±1.4	1.34±0.61
F5	86.2±1.2	1.37±0.44
F6	83.7±1.1	1.73±0.72
F7	88.0±1.3	1.66±0.68
F8	85.8±1.8	1.34±0.44
F9	83.2±2.0	1.51±0.66
F10	86.3±1.5	1.36±0.86
F11	82.9±1.3	1.74±0.53
F12	81.8±1.6	1.66±0.40
F13	83.1±1.0	1.54±0.46
F14	91.58±1.3	1.64±0.32
F15	88.2±1.2	1.77±0.41

the molecules are more mobile. This led to the development of resveratrol-loaded Solid Lipid Nanoparticles (SLN) and X-ray diffraction investigations (X-RD) for the medication (Figure 5). The diffraction spectra of pure resveratrol showed that the compound had crystallised.

Anti-Inflammatory Activity

If the two values, bp and cp are both less than 0.001, indicating a significant difference from the control group, then each reported value will represent the mean accompanied by the Standard Error of the Mean (SEM). The readings provided represent the average of triplicates, and the percentage Figures were calculated based on a range of concentrations of the experimental substances used for testing purposes. The statistical significance of the differences observed when compared to the control group is highlighted by the values of bp and cp being below the threshold of 0.001.

This demonstrates the precision of the measurements and the reliability of the reported data.

Inhibition of Protein Denaturation

Resveratrol SLN and Resveratrol Pure Drug successfully prevented heat-induced protein denaturation, according to this study's findings. Table 4 demonstrates that Resveratrol Pure Drug and Resveratrol SLN exhibited a 55.41% and 77.82% inhibition, respectively, with a significant (p<0:001), whereas diclofenac sodium at 500 µg/mL resulted in an 81.48% inhibition.

Assay of Cyclooxygenase

The impact of Resveratrol SLN and Resveratrol Pure Drug on prostaglandin synthesis was investigated by cyclooxygenase activity evaluation. Resveratrol Pure Drug, Resveratrol SLN, and Diclofenac sodium all substantially suppressed the cyclooxygenase activity at 500 µg/mL (p<0:001), with 63.06%, 80.58%, and 93.06%, respectively, according to Table 4.

Assay of 5-lipoxygenase

The drugs' effects on leukotriene generation were investigated by assessing 5-lipoxygenase activity. Table 4 shows that diclofenac sodium, Resveratrol SLN, and Resveratrol Pure Drug all significantly reduce 5-lipoxygenase activity (p<0:001), with 67.64%, 81.15%, and 91.36% of the activity, respectively.

Stability Study

Over the course of three months, the optimised formulation SLN F3 was subjected to two conditions: 25°C±2°C / 60% RH±5% RH and 40°C±2°C / 75% RH±5% RH. The parameters being studied were appearance, particle size, zeta potential, and encapsulation efficiency. Table 5 shows that SLN F3 was consistent for the first month, but that the formulation altered somewhat during the second and third months, but not considerably. A faint yellowish hue replaced the milky one. Although the zeta potential did not vary much, the entrapment efficiency dropped dramatically as the particle size rose slowly. At a temperature of 40°C±2°C and a relative humidity of 75%±5%, the SLN F3 took on a pinkish hue and the liquid become gooey after three months. In comparison

Table 4: Effect of Resveratrol Pure Drug and Resveratrol SLN (Optimized Formulation) with Standard sample Diclofenac Sodium on protein denaturation, Cyclooxygenase (COX), and 5-Lipoxygenase (LOX) inhibition.

Treatment	Dose (µg/mL)	Activity			Percent Inhibition		
		Protein Denaturation	COX	5-LOX	Protein Denaturation	COX	5-LOX
Control	-	-	-	-	-	-	-
Diclofenac Sodium	100	0:133±0:002[c]	0:011±0:44[c]	0:029±0:005[c]	81.48	93.06	91.36
Resveratrol Pure Drug	500	0:231±0:023[c]	0:037±0:003[c]	0:064±0:003[c]	55.41	63.06	67.64
Resveratrol SLN (Optimized Formulation)	500	0:115±0:003[c]	0:020±0:001[c]	0:038±0:009[c]	77.82	80.58	81.15

A significant difference relative to the control group (i.e., blank nanoparticles) is indicated by bp<0:001 and cp<0:001; measurements are given as the mean±SEM of triplicates.

Table 5: Stability Study Data of the Optimized Formulation.

25°C±2°C / 60% RH±5% RH				
Parameters	0 Day	30 Days	60 Days	90 Days
Appearance	Milky	Milky	Milky	Light Yellow
Particle Size	149.9±5.9 nm	151.4±6.2 nm	151.8±5.5 nm	152.4±8.5 nm
Zeta Potential	-30.9±2.6 mV	-30.9±3.6 mV	-30.4±2.1 mV	-31.7±8.4 mV
Entrapment Efficiency	91.8±1.7%	91.4±1.6%	90.8±1.5%	90.1±2.1%
40°C±2°C / 75% RH±5% RH				
Parameters	0 Day	30 Days	60 Days	90 Days
Appearance	Milky	Milky	Light Yellow	Pink
Particle Size	149.9±5.9 nm	154.6±4.8 nm	158.9±6.8 nm	162.8±9.7 nm
Zeta Potential	-30.9±2.6 mV	-31.4±2.8 mV	-31.8±3.4 mV	-32.4±7.6 mV
Entrapment Efficiency	91.8±1.7%	90.4±2.8%	88.5±2.7%	84.5±3.4%

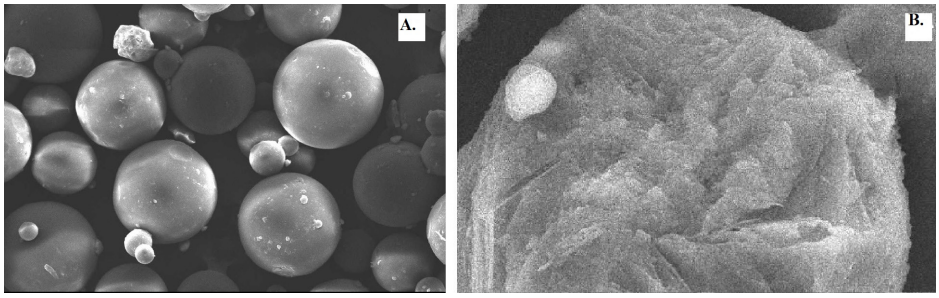

Figure 3: SEM of prepared SLN of resveratrol (Figure A represents the image from 200x magnification and Figure B represents the image from SEM at 3000x magnification.

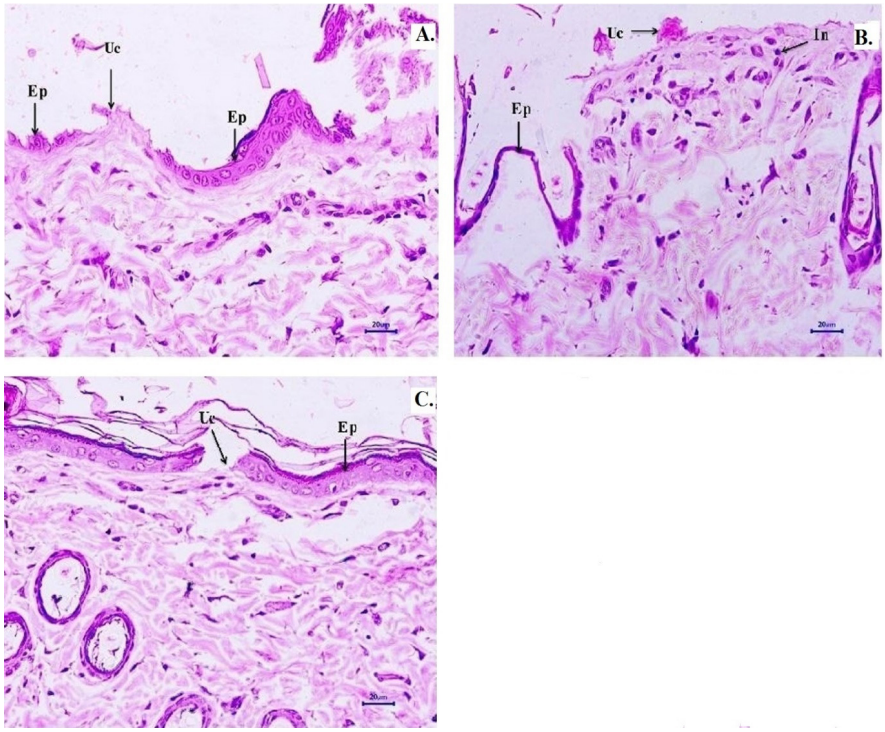

Figure 4: Histopathology of the intestine of Goat after the drug release study (Image A refers to pure drug and Image B refers to resveratrol loaded SLN).

to stability at 40°C±2°C / 75% RH±5% RH, the results showed that the SLN F3 formulation was more stable at 25°C±2°C / 60% RH±5% RH.

DISCUSSION

An increase in lipid content at a lower surfactant concentration was observed to have a substantial effect on particle size. The average formulation particle size grows in relation to the concentration of hydrogenated castor oil (Table 2). The surfactant solution may not have been able to stabilise the emulsion at the lowest concentration, which might explain this. The emulsion could be stabilised with a larger concentration of surfactant, maintaining a constant particle size, even when the lipid content was high. The particle size of the SLNs was found to be greatly altered by changing the surfactant concentrations. Table 2 shows that, holding lipid concentration constant, the particle size decreased as the lecithin concentration increased. The primary cause of this impact is the fact that the lecithin solution becomes more viscous. The impact of strong shear during emulsification causes a diminution in droplet size. Also, the surface energy is lowered because the droplets prefer to agglomerate. Nevertheless, the emulsion remains stable due to the surfactant molecules' ability to build a thick protective barrier around the droplets, preventing them from combining.

Particle size was decreased, and agglomeration was prevented more efficiently when soya lecithin and span 80 were combined, thanks to their synergistic impact. Predictions on the stability of colloidal dispersion can be made by measuring the Zeta Potential (ZP). As indicated in Table 2, the ZP of the SLNs had a negative surface charge because, as previously mentioned, the change in the ZP did not significantly vary with a change in either of the operational factors. These deductions make it easy to draw conclusions on the long-term stability of the distribution.

Combining soya lecithin and span 80 effectively decreased particle size and prevented agglomeration. The Zeta Potential (ZP) of

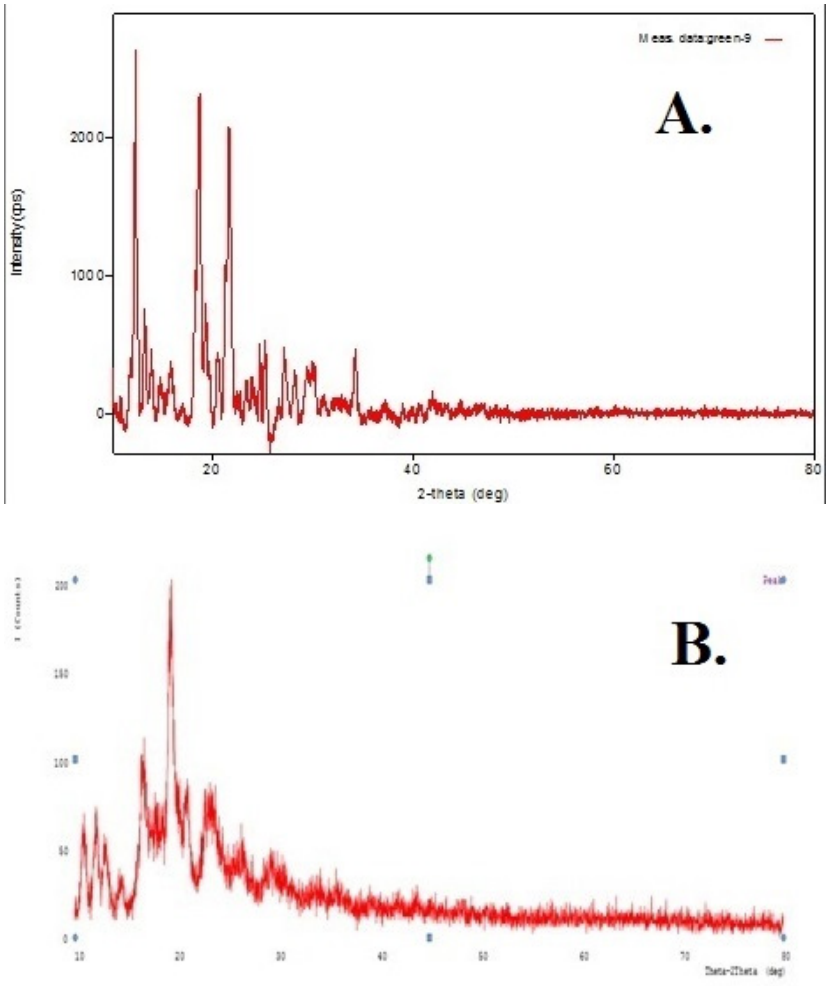

Figure 5: a) XRD of pure drug, b) XRD of drug loaded SLN.

SLNs showed a negative surface charge, indicating long-term stability of the distribution, despite changes in operational factors.

The occurrence might be attributed to either a reduction in nanoparticle size or an increase in the concentration of oleic acid. High pressure homogenization followed by low temperature solidification was the initial step in preparing the nanoparticles. Since solid lipids have a greater melting point than liquid lipids, they solidify quickly during low-temperature solidification, resulting in a solid lipid core with a randomly dispersed distribution of liquid lipids. A drug-enriched shell associated with drug burst release in the first stage results from a larger concentration of liquid lipids, which, in addition to being dispersed in the solid lipid core, would be positioned at the outer shell of the nanoparticles. Drug release rate was further enhanced because, when liquid lipid was spread into solid lipid, the crystalline structure of SLN became more defective, allowing pharmaceuticals loaded to be released more easily. Second, its size was diminutive.

The study focuses on the use of resveratrol-loaded Solid Lipid Nanoparticles (SLN) in enhancing drug delivery. The SLN formulation outperformed pure resveratrol in *ex vivo* permeation experiments, with a release rate of 76.65±1.58% after 24 hr. The formulation's diffusion through the medium significantly impacts the active ingredient's release rate. The lipid nanoparticles added to the SLN formulation made the substrate more lipophilic, indicating a greater affinity for the nanoparticles. The drug release mechanism was determined using mathematical models and X-ray diffraction. The SLN F3 formulation was stable under two conditions for three months. The drugs' effects on prostaglandin synthesis were also investigated, with Resveratrol Pure Drug, Resveratrol SLN, and Diclofenac sodium all significantly suppressing cyclooxygenase activity at 500 µg/mL. The drugs' effects on leukotriene generation were also assessed, with diclofenac sodium, Resveratrol SLN, and Resveratrol Pure Drug all significantly reducing 5-lipoxygenase activity.

CONCLUSION

The Solid Lipid Nanoparticles (SLN) encapsulating resveratrol were meticulously crafted using a reliable manufacturing technique known as high-pressure homogenization. This method

ensured the stability and efficiency of the SLN formulations. By showcasing a sustained-release profile, the SLN exhibited the ability to extend the drug's effects over an extended period, thereby enabling a reduced regimen frequency for dosing. Through a systematic analysis, this research substantiated the anti-inflammatory properties of the SLN in an *in vitro* setting. Various assays focusing on protein denaturation, cyclooxygenase, and 5-lipoxygenase inhibition presented a comprehensive evaluation of the anti-inflammatory efficacy of both the pure drug and the resveratrol-loaded SLN. Remarkably, the findings of this investigation underscored the potential of SLN as a promising carrier for facilitating the oral delivery of resveratrol as an adjuvant with synthetic NSAIDS.

ACKNOWLEDGEMENT

The authors express heartfelt gratitude towards the management of GH Raisoni University for their unwavering support and provision of essential facilities that enabled the successful execution of this project. Additionally, immense appreciation is extended to Nishika Labs for their invaluable assistance in conducting detailed DSC and SEM studies, which significantly contributed to the depth and accuracy of our research findings. The collaboration with these institutions played a pivotal role in enhancing the overall quality and comprehensiveness of this project, highlighting the importance of strong partnerships in academic endeavors.

ABBREVIATIONS

SLN: Solid Lipid Nanoparticles; **COX:** Cyclooxygenase; **PDI:** Polydispersity Index; **LOX:** Lipoxygenase; **FTIR:** Fourier Transmission Infra-red; **DSC:** Differential Scanning Caloreimetry; **SEM:** Scanning Electron Microscopy; **ZP:** Zeta Potential; **XRD:** X-ray Diffraction.

CONFLICT OF INTEREST

The authors declare that there is no conflict of interest.

SUMMARY

This study investigates an oral formulation of resveratrol and solid lipid nanoparticles. The formulation was prepared using oleic acid as a surfactant and hydrogenated castor oil as the lipid matrix. FTIR and DSC techniques were used to study drug interaction and physicochemical properties. *In vitro* anti-inflammatory tests were conducted using the Cyclooxygenase and 5-lipoxygenase method. A stability study was conducted, and the optimized formulation showed good stability and sustained release impact. The results suggest resveratrol in oral formulations may be more effective and less frequent.

REFERENCES

1. Pandey S, Shaikh F, Gupta A, Tripathi P, Yadav JS. A recent update: solid lipid nanoparticles for effective drug delivery. Advanced Pharmaceutical Bulletin. 2022; 12(1): 17.
2. Mirchandani Y, Patravale VB, Brijesh S. Solid lipid nanoparticles for hydrophilic drugs. Journal of Controlled Release. 2021; 335: 457-64.
3. Karunakar G, Patel NP, Kamal SS. Nano structured lipid carrier based drug delivery system. J Chem Pharm Res. 2016; 8(2): 627-43.
4. Harish V, Mohd S, Tewari D, Pandey NK, Vishwas S, Babu MR, *et al.* Unravelling the role of solid lipid nanoparticles in drug delivery: Journey from laboratory to clinical trial. Journal of Drug Delivery Science and Technology. 2023; 85: 104616.
5. Jannin V, Musakhanian J, Marchaud D. Approaches for the development of solid and semi-solid lipid-based formulations. Advanced drug delivery reviews. 2008; 60(6): 734-46.
6. Rezhdo O, Speciner L, Carrier R. Lipid-associated oral delivery: Mechanisms and analysis of oral absorption enhancement. Journal of Controlled Release. 2016; 240: 544-60.
7. Kathe N, Henriksen B, Chauhan H. Physicochemical characterization techniques for solid lipid nanoparticles: principles and limitations. Drug development and industrial pharmacy. 2014; 40(12): 1565-75.
8. Fuloria S, Sekar M, Khattulanuar FS, Gan SH, Rani NN, Ravi S, *et al.* Chemistry, biosynthesis and pharmacology of viniferin: potential resveratrol-derived molecules for new drug discovery, development and therapy. Molecules. 2022; 27(16): 5072.
9. Farhan M, Rizvi A. The pharmacological properties of red grape polyphenol resveratrol: Clinical trials and obstacles in drug development. Nutrients. 2023; 15(20): 4486.
10. Singh C, Rao K, Yadav N, Bansal N, Vashist Y, Kumari S, *et al.* A Review: Drug Excipient Incompatibility by FTIR Spectroscopy. Current Pharmaceutical Analysis. 2023; 19(5): 371-8.
11. González R, Peña MÁ, Torres NS, Torrado G. Design, development, and characterization of amorphous rosuvastatin calcium tablets. PLoS One. 2022; 17(3): e0265263.
12. Hammad SF, Rady MM, El-Malla SF. UV spectrophotometric methods for simultaneous determination of ketorolac tromethamine and olopatadine hydrochloride: Application of multiple standard addition for assay of ophthalmic solution. Scientific Reports. 2023; 13(1): 18143.
13. Aksoy OA, ZanbakÇotaoğlu M, Fatsa T, Topal GR, Eşim Ö, Göksel BA, *et al.* Preparation of Piroxicam nanosuspensions by high pressure homogenization and evaluation of improved bioavailability. Drug Development and Industrial Pharmacy. 2023; 49(12): 715-22.
14. Xie S, Pan B, Wang M, Zhu L, Wang F, Dong Z, *et al.* Formulation, characterization and pharmacokinetics of praziquantel-loaded hydrogenated castor oil solid lipid nanoparticles. Nanomedicine. 2010; 5(5): 693-701.
15. Yan T, Wang H, Song X, Yan T, Ding Y, Luo K, *et al.* Fabrication of apigenin nanoparticles using antisolvent crystallization technology: A comparison of supercritical antisolvent, ultrasonic-assisted liquid antisolvent, and high-pressure homogenization technologies. International Journal of Pharmaceutics. 2022; 624: 121981.
16. Aranda-Barradas ME, Trejo-López SE, Del Real A, Álvarez-Almazán S, Méndez-Albores A, García-Tovar CG, *et al.* Effect of molecular weight of chitosan on the physicochemical, morphological, and biological properties of polyplex nanoparticles intended for gene delivery. Carbohydrate polymer technologies and applications. 2022 Dec 1; 4: 100228.
17. Hongsa N, Thinbanmai T, Luesakul U, Sansanaphongpricha K, Muangsin N. A novel modified chitosan/collagen coated-gold nanoparticles for 5-fluorouracil delivery: Synthesis, characterization, *in vitro* drug release studies, anti-inflammatory activity and *in vitro* cytotoxicity assay. Carbohydrate Polymers. 2022; 277: 118858.
18. De Hoon I, Boukherroub R, De Smedt SC, Szunerits S, Sauvage F. *In vitro* and *ex vivo* models for assessing drug permeation across the Cornea. Molecular Pharmaceutics. 2023; 20(7): 3298-319.
19. Aggarwal S, Ikram S. Zinc oxide nanoparticles-impregnated chitosan surfaces for covalent immobilization of trypsin: stability & kinetic studies. International Journal of Biological Macromolecules. 2022; 207: 205-21.
20. Gupta RD, Raghav N. Nano crystalline cellulose based drug delivery system for some non-steroidal anti-inflammatory drugs: Synthesis, characterization and *in vitro* simulation studies. International Journal of Biological Macromolecules. 2023; 243: 124983.
21. Shitu IG, Katibi KK, Taura LS, Muhammad A, Chiromawa IM, Adamu SB, *et al.* X-ray diffraction (XRD) profile analysis and optical properties of Klockmannite copper selenide nanoparticles synthesized via microwave assisted technique. Ceramics International. 2023; 49(8): 12309-26.
22. Viji V, Helen A. Inhibition of lipoxygenases and cyclooxygenase-2 enzymes by extracts isolated from *Bacopa monniera* (L.) Wettst. Journal of ethnopharmacology. 2008; 118(2): 305-11.
23. Ballo M, Traore K, Guindo AD, Diakite SA, Dackouo B, Ouedraogo R, et al. *In vitro* inhibition of cyclooxygenases, anti-denaturation and antioxidant activities of Malian medicinal plants. African Journal of Pharmacy and Pharmacology. 2023; 17(2): 34-42.
24. Alhakamy NA, Hosny KM, Aldryhim AY, Rizg WY, Eshmawi BA, Bukhary HA, *et al.* Development and optimization of ofloxacin as solid lipid nanoparticles for

enhancement of its ocular activity. Journal of Drug Delivery Science and Technology. 2022; 72: 103373.

25. Bibi M, ud Din F, Anwar Y, Alkenani NA, Zari AT, Mukhtiar M, *et al.* Cilostazol-loaded solid lipid nanoparticles: Bioavailability and safety evaluation in an animal model. Journal of Drug Delivery Science and Technology. 2022; 74: 103581.
26. Chinchole A, Poul B, Panchal C, Chavan D. A review on stability guidelines by ICH and USFDA guidelines for new formulation and dosage form. PharmaTutor. 2014; 2(8): 32-53.
27. Silva AC, Kumar A, Wild W, Ferreira D, Santos D, Forbes B. Long-term stability, biocompatibility and oral delivery potential of risperidone-loaded solid lipid nanoparticles. International journal of pharmaceutics. 2012; 436(1-2): 798-805.

Cite this article: Malviya V, Khan A, Padole S, Thakre V, Gajbhiye T. Solid Lipid Nanoparticles of Resveratrol: Formulation, Characterization and *in vitro* Anti-Inflammatory Studies. Indian J of Pharmaceutical Education and Research. 2026;60(1):270-82.